RSC Advances

PAPER

View Article Online
View Journal | View Issue

Cite this: *RSC Adv.*, 2025, **15**, 16375

Effects of short-term thermal oxidation on the mechanical and thermal behavior of PA6 liner material for type IV hydrogen storage cylinders†

Xinshu Li,[ab] Qing Wang, *[a] Dongyang Wu,[a] Tingqu Li,[b] Peng Zhang,[a] Jingru Bai[a] and Xu Zhang[b]

The purpose of this study is to understand the changes in the performance of polyamide 6 (PA6) as a liner material under short-term thermal oxidation conditions. PA6 samples were subjected to oxidation at temperatures ranging from 90–150 °C for durations between 5–20 hours. Tensile, bending, and impact tests were conducted to evaluate changes in mechanical properties, while thermal analyses, including Fourier Transform Infrared Spectroscopy (FTIR), Thermogravimetric Analysis (TGA), and Differential Scanning Calorimetry (DSC), were performed to explore thermal stability and crystallization behavior. The results revealed that short-term thermal oxidation significantly influenced the ductility, tensile strength, and impact resistance of PA6, with marked decreases in these properties under higher oxidation temperatures and prolonged oxidation times. The material showed a clear embrittlement transition at 150 °C, with notable declines in tensile elongation and impact strength. The formation of carbonyl groups, particularly aldehydes and ketones, was accelerated by increased oxidation temperature and time, suggesting a correlation between thermal oxidation and chemical aging. Thermal analysis demonstrated a decline in thermal stability, characterized by reduced initial decomposition temperature ($T_{d5\%}$), maximum decomposition rate temperature (T_{dmax}), and end decomposition temperature (T_{end}) with increased oxidation severity. Meanwhile, crystallinity and melting enthalpy increased due to partial recrystallization during the oxidation process. These findings highlight the sensitivity of PA6 to thermal oxidation, underlining the importance of controlling oxidative conditions to maintain material performance. The study suggests the necessity for thermal management strategies and antioxidant incorporation to enhance the durability of PA6 for hydrogen storage applications, where exposure to elevated temperatures is inevitable.

Received 31st March 2025
Accepted 25th April 2025

DOI: 10.1039/d5ra02224j

rsc.li/rsc-advances

1 Introduction

With the global promotion of fuel cell vehicles,[1–4] Type IV hydrogen storage cylinders, as the most promising hydrogen storage devices, are receiving widespread attention.[5–8] Due to the unique structure of Type IV hydrogen storage cylinders, the liner material must not only possess high hydrogen barrier properties and thermal stability,[9–11] but also demonstrate excellent mechanical performance to withstand potential cracking and other failure modes during the hydrogen storage process.[12–15] The carbon fiber winding process tightly bonds the liner to the carbon fiber layer, requiring the liner material to have sufficient strength and toughness to resist challenges from pressure fluctuations and stress concentration.[16–19] Polyamide 6 (PA6), due to its outstanding mechanical properties and good chemical resistance,[20–23] has become a key material for the liners of Type IV hydrogen storage cylinders.

A considerable body of research has been dedicated to uncovering the performance evolution mechanisms of PA6 under long-term thermal oxidation conditions.[24–26] Forsström *et al.*[27,28] conducted early systematic studies on the thermal oxidation discoloration mechanisms and stability of polyamide 6, using chemical analysis techniques to determine changes in the key functional groups during the thermal oxidation process, and proposed a comprehensive degradation mechanism. Shu *et al.*[29] further investigated the long-term thermal oxidation behavior of PA6 within the temperature range of 110–150 °C, finding that crosslinking reactions in the early stages of oxidation enhanced mechanical strength. However, as the oxidation reaction continued, molecular degradation led to a gradual decline in mechanical performance. Dong *et al.*[30] used various characterization techniques to compare the thermal oxidation

[a]*Engineering Research Centre of Oil Shale Comprehensive Utilization, Ministry of Education, Northeast Electric Power University, Jilin 132012, Jilin, PR China. E-mail: rlx888@126.com*

[b]*School of Mechanical and Electrical Engineering, Jilin Institute of Chemical Technology, Jilin 132022, Jilin, PR China*

† Electronic supplementary information (ESI) available. See DOI: https://doi.org/10.1039/d5ra02224j

degradation processes of PA6 materials at temperatures ranging from 120 °C to 170 °C. Shi *et al.*[31] found that the thermal oxidation performance of highly oriented PA6 materials at 150 °C was independent of molecular orientation, but that a stable crystalline structure could significantly improve the material's gas barrier properties. Pliquet *et al.*[32] conducted a multi-scale, systematic study of the thermal oxidation characteristics of polyamide 6.6 in the temperature range of 140–200 °C, providing a comprehensive assessment from molecular to macroscopic levels. Additionally, significant progress has been made in the study of the thermal oxidation of PA6 composites.[21,33] For instance, Alexis *et al.*[34] investigated the performance changes of PA6/PA6.6 composites with different glass fiber contents after undergoing 500 hours of air-circulation thermal oxidation at 200 °C, revealing the degradation mechanisms of the composites in long-term high-temperature oxidative environments. These studies demonstrate the significant impact of thermal oxidation on the mechanical properties of PA6 materials. However, existing research has primarily focused on the effects of long-term thermal oxidation, with relatively limited studies on the impact of short-term thermal oxidation on the mechanical properties of PA6, particularly in hydrogen storage applications.

During the manufacturing process of Type IV hydrogen storage cylinders, the curing of the carbon fiber winding layer is typically achieved using heat-cured epoxy resin, which leads to short-term thermal oxidation of the liner material. To better understand the impact of this thermal oxidation on the performance of the PA6 liner material, this study aims to systematically evaluate the effects of short-term thermal oxidation on the mechanical and thermal properties of PA6, in order to explore its feasibility for use in Type IV hydrogen storage cylinders. Specifically, a series of experiments will be conducted to investigate the changes in tensile strength, flexural strength, impact toughness, thermal performance, and microstructural characteristics of PA6 under different short-term thermal oxidation conditions. Various techniques, including Fourier Transform Infrared Spectroscopy (FTIR), Scanning Electron Microscopy (SEM), Thermogravimetric Analysis (TGA), and Differential Scanning Calorimetry (DSC), will be employed to comprehensively reveal the effects of the thermal oxidation process on the material's chemical structure and performance. Through in-depth analysis of the experimental data, the study aims to provide theoretical support for optimizing PA6 materials and their application in hydrogen storage, laying a scientific foundation for the future development of hydrogen storage technologies.

The innovation of this study lies in its focus on the effects of short-term thermal oxidation on the performance of PA6 materials, complementing traditional long-term aging studies. In the context of the growing demand for efficient and safe hydrogen storage systems in fuel cell vehicles, this research will provide important scientific foundations for developing more durable and high-performance liner materials for Type IV hydrogen storage cylinders. It will also offer new insights into the behavior of materials during the carbon fiber winding process, contributing to the further application and development of hydrogen energy technologies.

2 Experimental

2.1 Materials

This study uses commercial-grade polyamide 6 pellets produced by Hunan Yuehua Company, model YH800. The material has the following characteristics: a density of 1.156 g cm^{-3}, a relative viscosity of 2.85 ± 0.03, a shrinkage rate of 0.93%, a melting point of 220 °C, and a heat distortion temperature of 71 °C. These parameters provide a basis for analyzing the changes in the mechanical properties and thermal performance of PA6 under short-term thermal oxidation conditions.

2.2 Sample preparation

The material used in this study consists solely of PA6. To meet the requirements for mechanical property testing, the PA6 pellets were injection-molded into different sizes. Due to the hygroscopic nature of PA6, the required pellets were vacuum-dried at 105 °C for 8 hours before injection molding. The mechanical specimens were molded using the PNX40III-2A micro-sample preparation system produced by NESSI Plastic Industrial Co. Ltd. The injection molding standards and dimensions of the specimens are shown in Table 1. The mold temperature was kept moderate, around 80 °C, while the melt temperature of the PA6 pellets was controlled between 240–250 °C. High-speed injection was performed with an injection pressure of 120 MPa, followed by a pressure holding time of 2 seconds, with the holding pressure reduced by half. Additionally, the PA6 pellets were ground to a mesh size of 100, and a portion of the powder was used for thermal oxidation treatment. The samples were subjected to thermal oxidation using an air-circulation oven, with the oxidation temperature controlled between 90–150 °C and the oxidation time limited to 20 hours. Samples were taken every 5 hours, and the mechanical specimens after thermal oxidation are shown in Fig. 1.

2.3 Instrument and measurement

Tensile and bending tests were conducted using the WAW-E microcomputer-controlled electronic universal testing machine (manufacturer: Jinan Meters Testing Technology Co., Ltd), with a frequency of 50 Hz, a maximum load capacity of 20 kN, and a precision grade of 0.5. The tensile tests followed the ISO 527 standard, with a testing speed of 10 mm min^{-1}, using dog-bone-shaped specimens with a gauge length of 50 mm to ensure that fracture occurred within the gauge length range. At least 5 valid data points were obtained for each group of specimens. Bending tests were conducted according to the ISO 178 standard, with a displacement speed of 5 mm min^{-1}, a span of 48 mm, and a displacement maintained at 20 mm for 5 seconds, followed by a stop. At least 5 valid data points were obtained for each group of specimens. Notched impact strength was tested using the ZwickRoell pendulum impact testing machine, with friction loss determined through blank impact tests, and the final impact energy results were corrected. Each group of

Table 1 Injection molding standards and dimensions of mechanical specimens

Sample name	Standard	Size
Tensile specimen	ISO527-2-2012	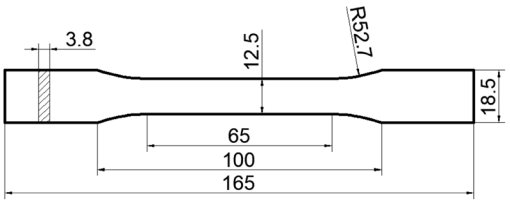
Bending specimen	ISO178	
Impact specimen	ISO180	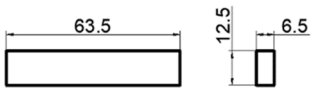

specimens ensured at least 5 valid data points. All tensile, bending, and impact strength tests were performed under standard climate conditions (23 °C, 50% relative humidity).

The Fourier transform infrared (FTIR) spectrometer (PerkinElmer, USA) was used to measure the functional groups in the thermally oxidized PA6 powder. The spectral measurement range was 400–4000 cm^{-1}, with a resolution of 4 cm^{-1}, and 32 scans were conducted within the spectral range.

The scanning electron microscope (SEM, JSM-7610F, JEOL, Japan) was used to observe the morphology of the thermally oxidized PA6 material and to analyze the changes in the microstructure of PA6 before and after thermal oxidation.

Thermogravimetric analysis (TGA) was conducted using a thermogravimetric analyzer (TG; Mettler Toledo, Switzerland) on both unoxidized and thermally oxidized PA6 materials. Samples (8 ± 0.2 mg) were placed in crucibles and analyzed under a nitrogen flow at a heating rate of 10 °C min^{-1}, with the temperature range from 30 °C to 700 °C, to obtain the TG curve.

Differential scanning calorimetry (DSC; Mettler Toledo, Switzerland) was used to perform non-isothermal crystallization analysis on both unoxidized and thermally oxidized PA6 materials. Samples (8 ± 0.2 mg) were placed in crucibles and heated under a nitrogen flow at a rate of 10 °C min^{-1}, from 30 °C to 250 °C, where they were held for 5 minutes to eliminate thermal history effects. The temperature was then reduced at a rate of −10 °C min^{-1} from 250 °C to 30 °C to determine the crystallization temperature and crystallization enthalpy. Finally, the samples were heated again at 10 °C min^{-1} from 30 °C to 250 °C to obtain the melting temperature and melting enthalpy. The heat absorbed during the melting of PA6 material is nearly equal to the heat required to disrupt the crystal structure, and the degree of crystallinity (X_c) is positively correlated with the melting enthalpy (ΔH_m). The crystallinity is calculated using the following formula

$$X_c = \frac{\Delta H_m}{\Delta H_0} \times 100\%$$

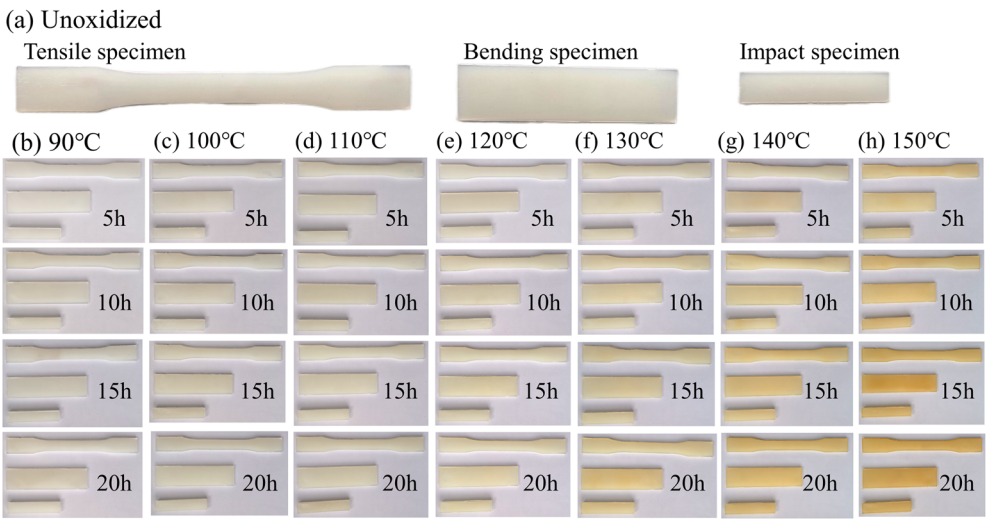

Fig. 1 Mechanical specimen diagram (a–h).

In this equation, ΔH_0 represents the standard melting enthalpy, which is the melting enthalpy of 100% crystalline PA6 material. According to the manufacturer's provided data, the standard melting enthalpy is 190 J g^{-1}.[29]

3 Results and discussion

3.1 Tensile properties analysis

In this section, based on the tensile test results, the tensile response of PA6 material samples subjected to thermal oxidation at temperatures ranging from 90 °C to 150 °C and for oxidation times between 5 and 20 hours is presented. The stress–strain curves for PA6 samples under four different thermal oxidation times (5 h, 10 h, 15 h, and 20 h) are shown in Fig. 2. The results are provided for comparison purposes only. Although each sample was tested multiple times to ensure accuracy and reproducibility, only one curve is shown for each condition in Fig. 2 to maintain clarity and conciseness in the graphical presentation.

From Fig. 2(a) with a thermal oxidation time of 5 hours and Fig. 2(b) with a thermal oxidation time of 10 hours, it can be observed that at thermal oxidation temperatures between 90 °C and 150 °C, the maximum tensile strength always occurs at the yield point. However, Fig. 2(c) (oxidation time of 15 hours) and Fig. 2(d) (oxidation time of 20 hours) indicate that the maximum tensile strength occurs at the yield point only when the oxidation temperature remains between 90 °C and 140 °C. In the elastic deformation phase, the stress and strain of the material have a linear relationship, with stress increasing gradually as the external force increases until it reaches the yield point, at which point the PA6 material experiences its maximum stress. During the elastic deformation stage, the microstructure of the PA6 material remains relatively intact, and the interactions between the molecular chains are strong enough to resist the increasing external force. However, once the yield point is reached, the internal structure of the PA6 material begins to deteriorate, and the stress ceases to increase. In the subsequent plastic deformation phase, the molecular chains of the PA6 material undergo relatively free slippage and breakage, causing the material to lose its ability to withstand further stress, which means that the stress will not surpass the yield point again.

When the thermal oxidation time was extended to 15 hours (Fig. 2(c)) and 20 hours (Fig. 2(d)), the tensile stress–strain curves at a higher oxidation temperature (150 °C) showed brittle fracture occurring directly during the elastic stage. In contrast, PA6 samples oxidized at lower temperatures (90–140 °C) exhibited ductile fracture. For PA6 samples with oxidation times

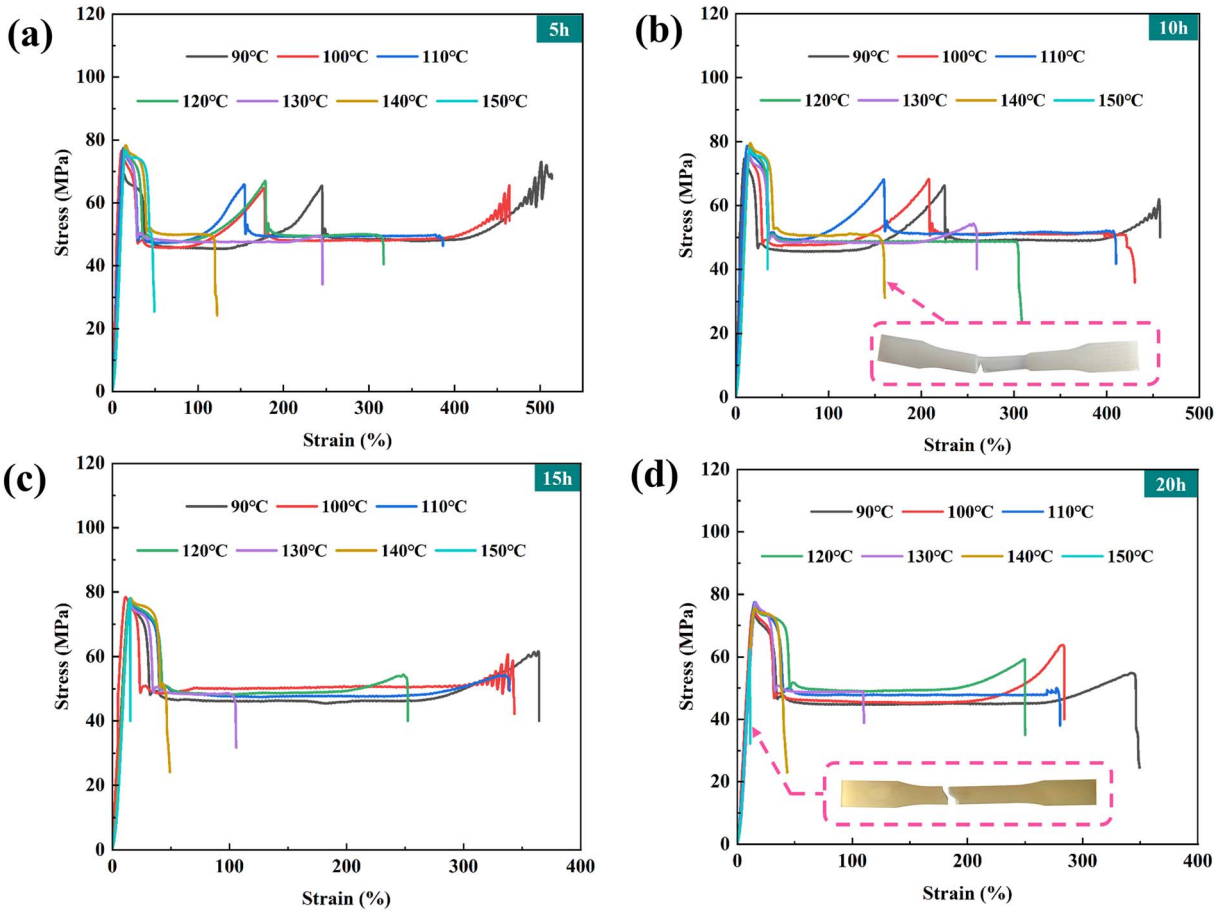

Fig. 2 Tensile stress–strain diagrams (a–d) under different thermal oxidation conditions.

of 5 and 10 hours, ductile fracture was observed at all thermal oxidation temperatures (90–150 °C).

PA6 is a long-chain polymer that exhibits a certain degree of disorder and curl in its unstressed state, with molecular chains randomly arranged to form a complex three-dimensional network structure. When an external force is applied, the molecular chains gradually straighten along the direction of tension. Under low-stress conditions, the chains begin to extend, which is known as the elastic region. In this phase, deformation is reversible, and small displacements of chain segments do not significantly change the intermolecular forces. The stretching of the molecular chains mainly relies on the balance of interactions such as van der Waals forces and hydrogen bonds between chain segments. As the external force increases, the molecular chains continue to unfold until a certain stress level is reached, known as the yield point, at which the material's internal microstructure starts to change. The slippage between chain segments gradually increases, forming slip planes, and the material enters the plastic deformation phase. In this phase, some regions of the chain segments are overstretched, resulting in localized reductions in cross-sectional area, known as necking. In the necked region, the arrangement of chain segments becomes more compact, causing increased stress concentration until fracture occurs.

For thermally oxidized PA6 materials, the weakening of chain segments makes fracture more likely to occur, resulting in a gradual decrease in elongation as the thermal oxidation temperature increases (Fig. 3). As the thermal oxidation temperature rises, the elongation of PA6 material decreases progressively (Table 2). Under the same thermal oxidation temperature, the longer the oxidation time, the lower the elongation at break of the PA6 material (Fig. 3 and Table 2).

Fig. 3(a) illustrates the trend in tensile elongation at break for PA6 material under different temperatures (90 °C to 150 °C) and various thermal treatment durations (5 h to 20 h). The *X*-axis represents the thermal oxidation temperature (°C), the *Y*-axis indicates the thermal oxidation duration (h), and the *Z*-axis shows the elongation (%) of the PA6 material. This 3D surface plot provides a clear visualization of the changes in elongation performance of PA6 under different thermal oxidation conditions. From the figure, it is evident that the elongation of PA6 material generally decreases as both the temperature and duration of the treatment increase. In particular, the elongation significantly decreases under high temperatures (above 130 °C) and relatively long durations (over 15 h), indicating that thermal oxidation has a substantial effect on the elongation performance of PA6, thereby leading to a significant reduction in the material's toughness. At lower temperatures (90 °C to 120 °C) and shorter durations (5 h), PA6 material exhibits relatively high elongation, exceeding 300%, suggesting that the toughness of the material remains largely unaffected under mild treatment conditions. This observation is consistent with the fact that the color change of PA6 samples under these conditions is minimal (Fig. 1). However, as the thermal oxidation temperature further increases to 150 °C and the duration exceeds 15 h, the elongation of PA6 material drops to approximately 10%, indicating that the material has nearly become completely brittle, likely due to severe molecular chain breakage.

Fig. 3(b) shows the retention rate of elongation for PA6 material under different thermal oxidation conditions. Under

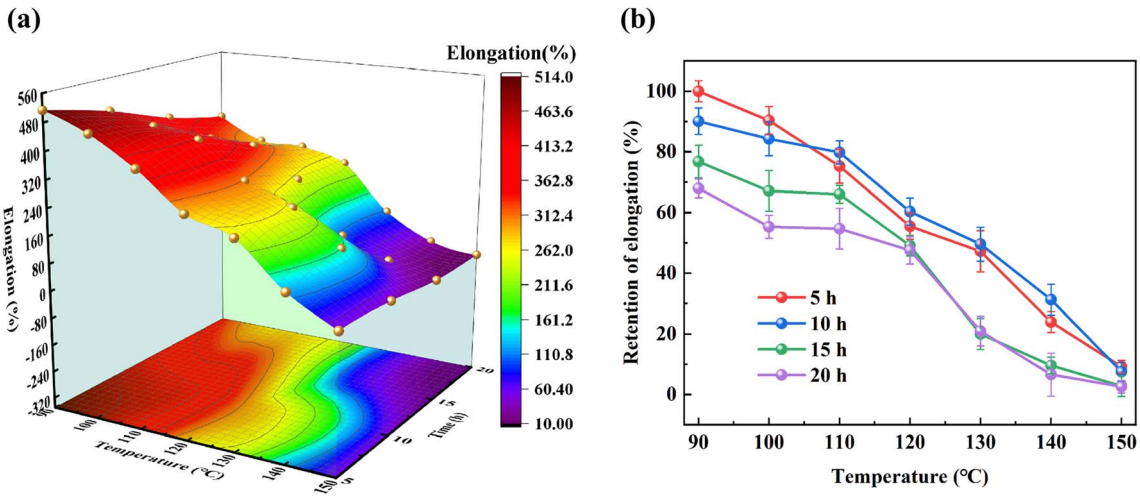

Fig. 3 (a) Elongation and (b) retention of elongation under different thermal oxidation conditions.

Table 2 Tensile strength, Young's modulus, elongation of the material measured in tensile test

Thermal oxidation condition	Tensile strength (MPa)	Young's modulus (MPa)	Elongation (%)	Bending strength (MPa)	Bending modulus (MPa)	Impact strength (MPa)
Unoxidized	72.9	2637.8	513.8	107.29	1846.4	41.91
150 °C, 20 h	69.6	2746.0	13.1	85.88	1826.1	3.16

thermal oxidation at 90 °C, the elongation retention rate for PA6 material after 5 hours of oxidation is 99.98%, after 10 hours it is 90.07%, after 15 hours it is 76.76%, and after 20 hours it is 67.96%. In contrast, under thermal oxidation at 150 °C, the elongation retention rate for PA6 material is below 10% for all oxidation times. These results indicate that under high-temperature conditions, thermal oxidation leads to the gradual degradation of polymer chains within the material, resulting in chain breakage that reduces chain segment mobility and significantly lowers the elongation of the material. On the other hand, under low-temperature conditions, the elongation of PA6 material is more significantly affected by the oxidation duration. PA6 is a semi-crystalline polymer, and its elongation properties are primarily influenced by the arrangement of molecular chains and the mobility of chain segments. Additionally, the oxidation process may lead to free radical reactions, further accelerating the aging and embrittlement of the material, especially under high-temperature and prolonged oxidation conditions.

From Fig. 4, which depicts the changes in tensile strength of PA6 material under different thermal oxidation temperatures and durations, it can be observed that the tensile strength of PA6 material exhibits a certain trend with increasing thermal oxidation temperature and extended duration. Under higher temperatures (110 °C to 140 °C) and intermediate durations (10 h to 15 h) of thermal oxidation, the tensile strength remains at a relatively high level. The maximum tensile strength of 79.6 MPa occurs under thermal oxidation at 140 °C for 10 hours. When the thermal oxidation temperature exceeds 130 °C and the duration exceeds 15 hours, the tensile strength starts to show a significant decline. The minimum tensile strength of 69.6 MPa is observed at a higher temperature (150 °C) and a longer duration (20 hours), which is about a 15% reduction compared to the maximum tensile strength. When the thermal oxidation time reaches 20 hours, the tensile strength retention rate first shows a gentle increase and then a rapid decline with increasing temperature, indicating that the temperature has the most significant impact. At an oxidation time of 15 hours, the tensile strength retention rate is the most stable (Fig. 4(b)). This suggests that high temperature combined with longer durations has a negative impact on the tensile properties of the material. In particular, when the temperature exceeds 130 °C, the thermal oxidation process intensifies the degradation of polymer chains, leading to a significant reduction in the tensile strength of PA6 material. This is consistent with the thermal oxidation aging mechanism of the material,[29] indicating that the toughness and overall structure of the material have been severely compromised.

Fig. 5 reflects the stiffness characteristics of the material, showing that the Young's modulus of PA6 material varies significantly under different thermal treatment conditions. However, as shown in Table 2, the trend of Young's modulus remains relatively stable across different thermal oxidation temperatures and durations, with only a slight decrease observed at higher temperatures and longer oxidation times.

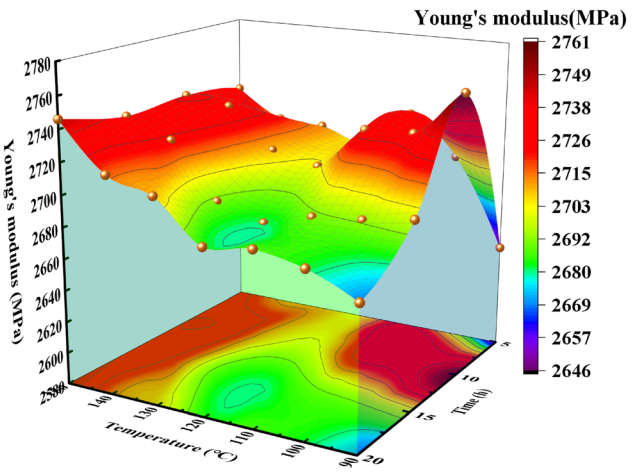

Fig. 5 Young's modulus under different thermal oxidation conditions.

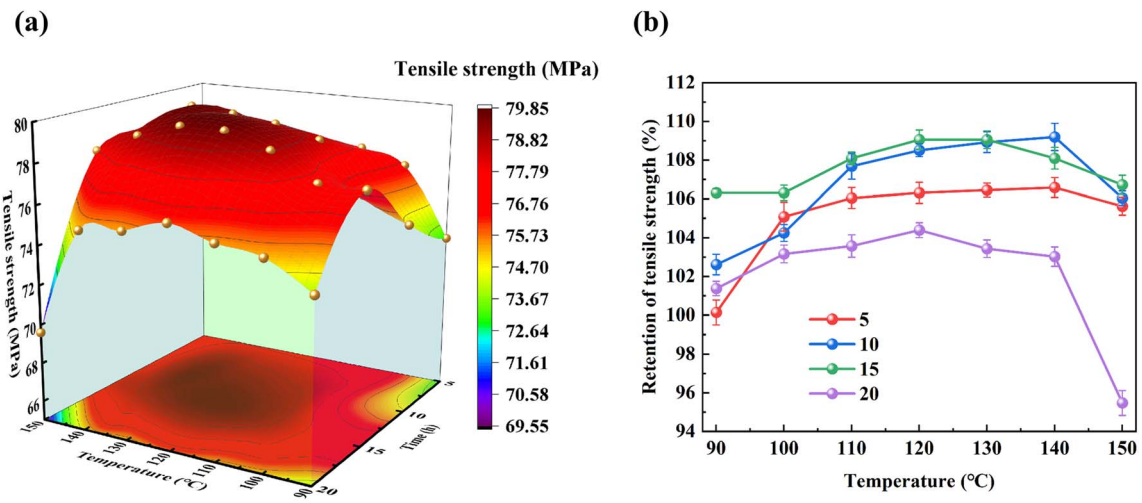

Fig. 4 (a) Tensile strength and (b) retention of tensile strength under different thermal oxidation conditions.

The difference between the maximum and minimum values is only about 3%.

Based on the analysis of the tensile performance test results of PA6 samples, it can be concluded that both temperature and time are key factors influencing the tensile properties of PA6 material under short-term thermal oxidation. As the thermal oxidation temperature increases, the material's ductility significantly decreases, while strength initially increases and then decreases, and changes in stiffness are relatively small. These observations align with the findings reported by Backens *et al.*[35] in their study on PA6 material aging, where tensile strength demonstrated an increasing trend post-aging, while Young's modulus exhibited no statistically significant variation.

3.2 Bending properties analysis

In this section, based on the bending test results, an analysis of the bending performance of PA6 material samples subjected to thermal oxidation at temperatures ranging from 90 °C to 150 °C and for oxidation times between 5 and 20 hours is presented. Fig. 6 shows the bending stress–strain curves of PA6 material after thermal oxidation at different temperatures (90 °C to 150 °C) for 5, 10, 15, and 20 hours. Analyzing the stress–strain curves under different thermal oxidation conditions is crucial for understanding the effects of oxidation time and temperature on the mechanical properties of PA6 material.

When the thermal oxidation treatment time was 5 hours (Fig. 6(a)) and 10 hours (Fig. 6(b)), the maximum bending stress of PA6 material remained between approximately 107–114 MPa, indicating that short-term thermal oxidation has a minimal impact on the bending strength of the material. The differences in maximum bending stress values at different temperatures (90 °C to 150 °C) were not significant (Fig. 7), suggesting that PA6 material maintains good mechanical stability during short-term thermal oxidation. After reaching the maximum stress, the stress began to gradually decrease, showing a trend of plastic deformation, indicating that PA6 material still retained good ductility and the ability for plastic deformation after thermal oxidation treatment, without exhibiting significant embrittlement. Additionally, although the descending part of the curve was slightly steeper at higher temperatures (150 °C), implying that higher temperatures may accelerate material failure, overall, the oxidation times of 5 to 10 hours were insufficient to significantly reduce the material's ductility (Fig. 6(a) and (b)).

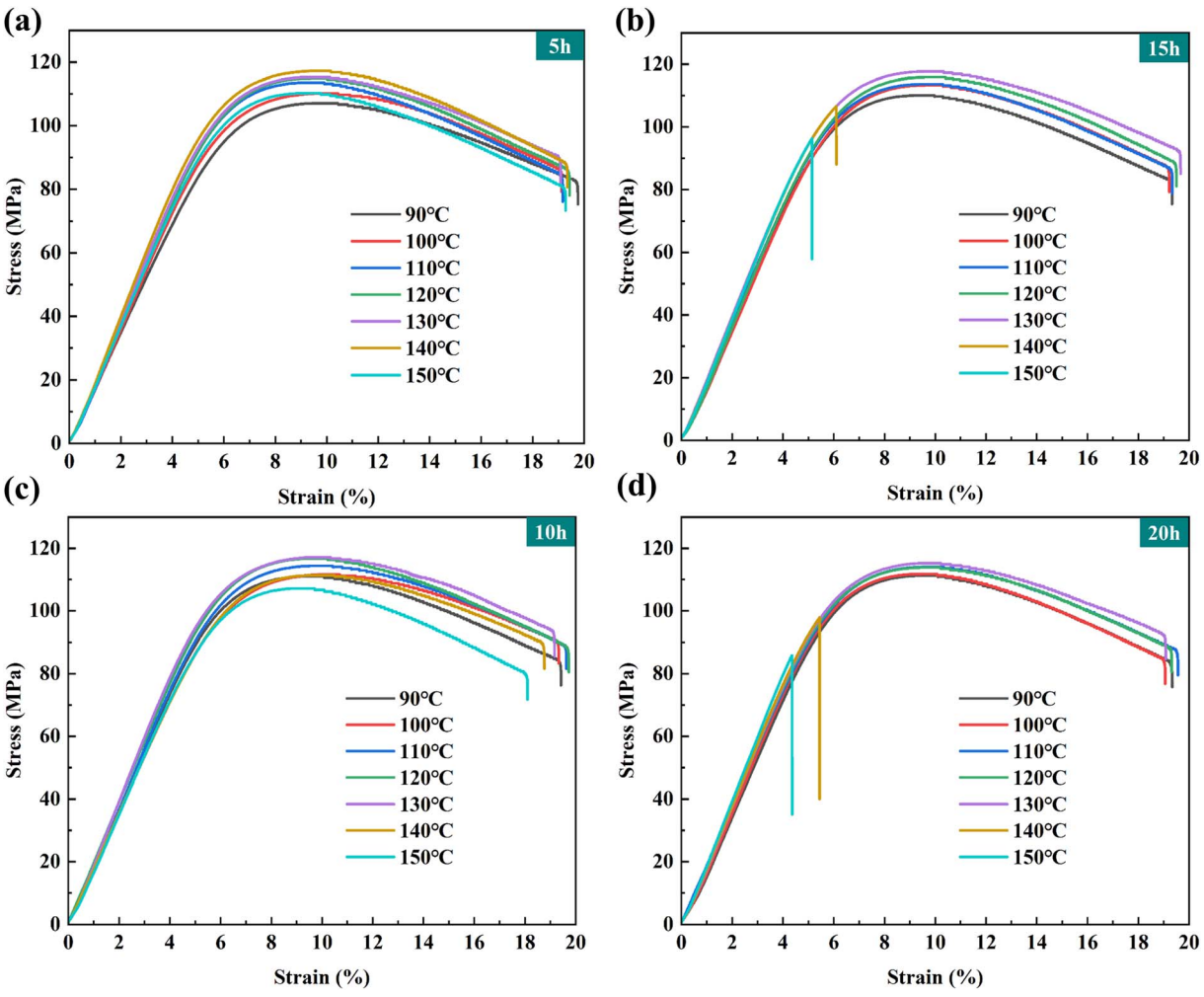

Fig. 6 Bending stress–strain diagrams (a–d) under different thermal oxidation conditions.

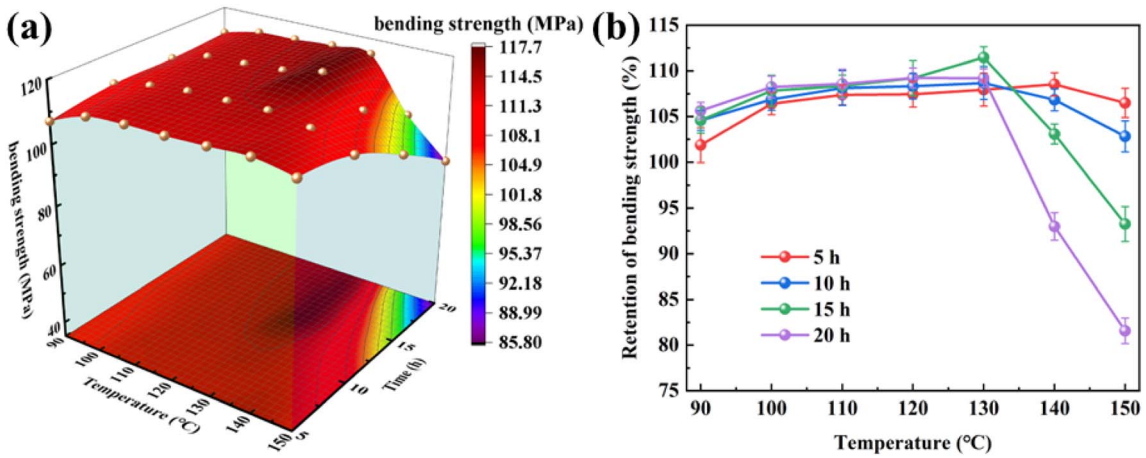

Fig. 7 (a) Bending strength and (b) retention of bending strength under different thermal oxidation conditions.

For the bending stress–strain curves after 15 hours of thermal oxidation (Fig. 6(c)), especially at higher temperatures (140 °C and 150 °C), the maximum stress of the material decreased significantly, indicating that the mechanical properties of PA6 material were progressively degraded with increased thermal oxidation time. As the oxidation temperature increased, the yield point appeared earlier, and the stress dropped rapidly, indicating a significant reduction in ductility and plasticity, along with increased brittleness. Moreover, the stress–strain curves for 15 hours of thermal oxidation showed early signs of fracture at higher temperatures, particularly at 140 °C and 150 °C, where some curves exhibited a marked decrease in stress. This phenomenon suggests that high temperature and extended oxidation accelerate the degradation and breakage of molecular chains within the material, increasing brittleness and making it more susceptible to failure at lower strain levels. The stress–strain curves after 20 hours of thermal oxidation (Fig. 6(d)) also exhibited pronounced brittle fracture, especially at higher temperatures (140 °C and 150 °C).

During thermal oxidation, the microstructure of PA6 material undergoes changes that directly affect its macroscopic mechanical properties. Thermal oxidation results in partial degradation and oxidation reactions of PA6 molecular chains, leading to the breakage of chemical bonds between polymer chains and the formation of oxidation products, such as carbonyl and hydroxyl groups. The accumulation of these oxidation products weakens the intermolecular forces, resulting in a decline in the rigidity and strength of the material. However, with a shorter oxidation time of 5 hours, the degree of molecular chain degradation is limited, and no significant embrittlement is observed. In contrast, under oxidation conditions exceeding 15 hours, the cumulative effects of degradation and oxidation become more pronounced, leading to a significant reduction in the material's mechanical properties, manifested as decreases in both strength and ductility.

The 3D surface plot of maximum bending strength in Fig. 7 further illustrates the effects of different thermal oxidation temperatures and durations on the mechanical properties of PA6 material. As temperature and time increase, the maximum bending strength shows an overall decreasing trend. Under lower temperatures and relatively short oxidation durations (90 °C, 5 hours), the maximum bending strength of the material is close to that of unoxidized PA6, reaching approximately 110 MPa. However, as the temperature increases to 150 °C and the oxidation time extends to 20 hours, the maximum bending strength drops significantly to around 85 MPa. A turning point occurs at a thermal oxidation temperature of 140 °C with an oxidation time of 20 hours, and at 150 °C with an oxidation time of 15 hours. This indicates that prolonged thermal oxidation at high temperatures significantly weakens the mechanical properties of the material. Under the same thermal oxidation temperature, a decline in bending strength is observed when the oxidation time reaches 20 hours, resulting in a smooth transition of the strength surface from higher to lower values. This trend suggests that even under low-temperature conditions, relatively long thermal oxidation durations can gradually damage the internal structure of the material, ultimately leading to deterioration in mechanical performance. In Fig. 7(b), the retention rate of bending strength remains stable for oxidation times of 5 and 10 hours, with retention rates exceeding 100%, indicating that the bending strength of the material is actually enhanced compared to unoxidized PA6. Additionally, for oxidation times of 15 and 20 hours, the retention rate remains stable and above 100% when the oxidation temperature is below 130 °C. However, when the temperature exceeds 130 °C, the retention rate of bending strength drops significantly, indicating a rapid decline in bending strength compared to unoxidized PA6 material.

The 3D surface plot of bending modulus (Fig. 8) further reveals the impact of thermal oxidation on the rigidity of PA6 material. As the thermal oxidation temperature increases, the bending modulus initially rises and then decreases. Under lower temperatures (90 °C), the bending modulus of PA6 material remains above 1850 MPa but does not exceed 1900 MPa. As the oxidation temperature rises to 130 °C, the modulus gradually increases, reaching a maximum value of 2068 MPa, which occurs at an oxidation duration of 10 hours. However, when the temperature continues to rise to 150 °C and

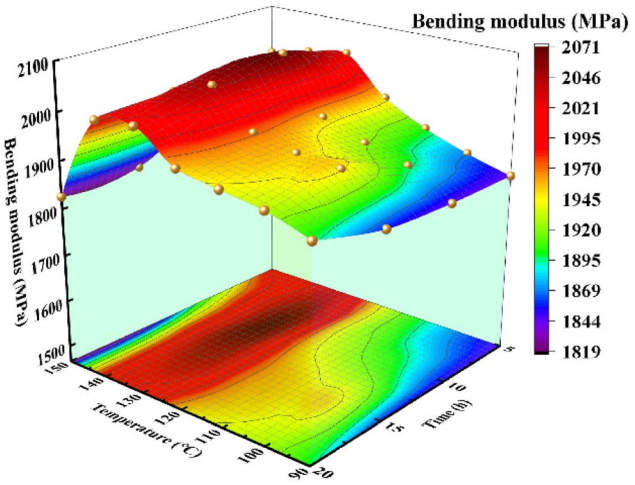

Fig. 8 Bending modulus under different thermal oxidation conditions.

the oxidation time extends to 15 hours, the bending modulus begins to decline significantly. This suggests that under prolonged and high-temperature thermal oxidation, the molecular chains of PA6 degrade, and chemical bonds break, leading to a reduction in material rigidity. As the thermal oxidation time extends to 20 hours, the bending modulus decreases under most thermal oxidation temperatures (100 °C to 150 °C), showing a smooth transition in the modulus surface from higher to lower values. This indicates that even under lower temperatures, long-term thermal oxidation treatment still causes damage to the internal structure of the material, ultimately leading to a decline in rigidity. However, the difference between the maximum and minimum values of the bending modulus for PA6 under different thermal oxidation conditions is only 9.7%, indicating that short-term thermal oxidation has a relatively minor effect on the stiffness of PA6 material.

In conclusion, thermal oxidation temperature and duration have a significant impact on the bending performance of PA6 material. In practical applications, it is essential to strictly control the environmental temperature and oxidation time to prevent material performance degradation and ensure its reliability during long-term use. These results indicate that PA6 exhibits good stability under short-term thermal oxidation; however, as oxidation time extends or temperature further increases, the material's mechanical properties are more adversely affected. Therefore, it is important to consider the potential impact of long-term high-temperature oxidation on material performance to ensure the reliability of PA6 in actual applications.

3.3 Impact properties analysis

Based on the impact test results, the effect of thermal oxidation on the toughness of PA6 material can be further revealed. As shown in Fig. 9, the impact strength decreases significantly as both temperature and oxidation time increase. Under lower temperatures (90 °C) and shorter durations (5 hours), the impact strength of PA6 remains high, at around 41.8 MPa, which is comparable to that of unoxidized PA6 material. However, when the temperature increases to 150 °C and the oxidation time extends to 20 hours, the impact strength drops sharply to 3.16 MPa, representing a decrease of approximately 92.4% compared to PA6 oxidized at 90 °C for 5 hours. The downward trend in impact strength indicates that thermal oxidation adversely affects the toughness of the material. Higher temperatures and longer oxidation durations lead to the breaking and degradation of molecular chains, weakening the material's ability to absorb impact energy, thus reducing its impact strength. Especially at higher temperatures (*e.g.*, 150 °C) and extended durations (*e.g.*, 20 hours), the material becomes more brittle, resulting in a significant decrease in impact strength. The research findings of Backens *et al.*[35] further corroborate the significant decline in impact strength of PA6 materials following aging. This consistency across independent studies underscores the critical relationship between oxidative aging and the embrittlement mechanism in polyamide systems. This observation aligns well with the tensile test analysis (Fig. 3), which also shows increased brittleness of PA6 material under prolonged high-temperature oxidation conditions.

From a molecular structural perspective, significant changes occur in the molecular chains of PA6 during thermal oxidation, resulting in a substantial reduction in impact strength. Under

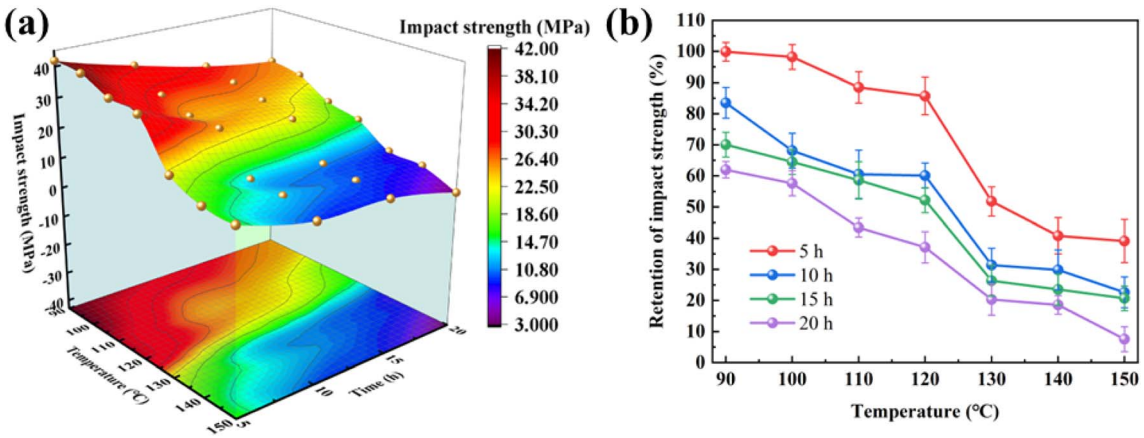

Fig. 9 (a) Impact strength and (b) retention of impact strength under different thermal oxidation conditions.

thermal oxidation conditions, the amide bonds (–CONH–) in the polyamide 6 molecular chains are prone to breaking, generating free radicals and leading to a decrease in molecular weight. Oxidation also causes the formation of oxidation products, such as carbonyl and hydroxyl groups, between chain segments, and the accumulation of these chemical groups can induce chain scission and crosslinking reactions. The breakage of chain segments weakens the flexibility of the material, making it more susceptible to brittle fracture under impact. Additionally, although crosslinking can increase material hardness to some extent, it also reduces flexibility, further impairing the material's ability to absorb impact energy. In summary, the degradation and crosslinking effects of molecular chains caused by thermal oxidation are the primary reasons for the significant reduction in PA6 impact strength. This mechanistic framework is supported by Backens *et al.*'s[35] study, which demonstrates that the fundamental vulnerability of the amorphous matrix of PA6 to embrittlement remains a consistent phenomenon even under different aging protocols. This generalization suggests that the degradation of impact properties is an intrinsic limitation of the PA6 chemical structure in aggressive environments rather than a product of specific aging protocols.

3.4 Molecular structure analysis

3.4.1 SEM. By comparing the morphology of the unoxidized and oxidized PA6 materials (Fig. 10 and S1†), it can be seen that the surface of the unoxidized PA6 is relatively smooth, with no obvious cross-linking or entanglement structure. The PA6 material treated with thermal oxidation at 130 °C can be observed to have a wrinkled surface, but no obvious "blistering" phenomenon was observed, and the PA6 material treated with thermal oxidation at 150 °C for 15 h can be observed to have the beginning of the "blistering" phenomenon. As the degree of thermal oxidation deepens, the PA6 material after 20 h of 150 °C thermal oxidation treatment, on the other hand, obvious surface wrinkles and "blistering" phenomenon. This "progressive" aging phenomenon indicates that the PA6 material is gradually accentuating its aging characteristics as the degree of thermal oxidation deepens. This indicates that after thermal oxidation treatment, PA6 material begins to exhibit signs of aging, with the previously stable molecular structure showing evidence of crosslinking and chain scission. These changes in the microstructure provide strong support for the previous findings regarding the decline in mechanical properties of thermally oxidized PA6 material. However, further exploration of this thermal oxidation phenomenon is required, which will be addressed in subsequent parts of the study.

3.4.2 FTIR. During the oxidation process of PA6, carbonyl compounds such as ketones and aldehydes are readily formed. Under suitable conditions, these carbonyl compounds can further oxidize to form additional carbonyl-containing compounds, such as hydroxy acids. To compare the chemical structural changes of PA6 material under different thermal oxidation conditions, the infrared spectra are shown in Fig. 10. The FTIR spectra in this study exhibit distinct characteristic peaks, as shown in Fig. 11(a), which describes the infrared spectra of PA6 at 150 °C under different thermal oxidation durations. Specifically, the characteristic absorption band of CO–NH, associated with hydrogen bonding, appears as a carbonyl band at 1710–1780 cm^{-1} (C=O stretching vibration), and its intensity increases with longer oxidation time (Fig. 11(b)). In contrast, the absorption peaks corresponding to the amine bands at 3300–3400 cm^{-1} (N–H stretching vibration) and 1550–1650 cm^{-1} (N–H bending), as well as the methylene bands at 2800–3000 cm^{-1} (C–H stretching vibration), gradually decrease in intensity as the oxidation time extends (Fig. 11(a)).[27,30,31] These changes reveal the reasons for the observed decline in mechanical properties, particularly the decrease in impact strength, following the thermal oxidation of PA6. The variations in these peaks indicate that PA6 material undergoes aging during thermal oxidation, and regardless of changes in oxidation conditions, the aging mechanism of the

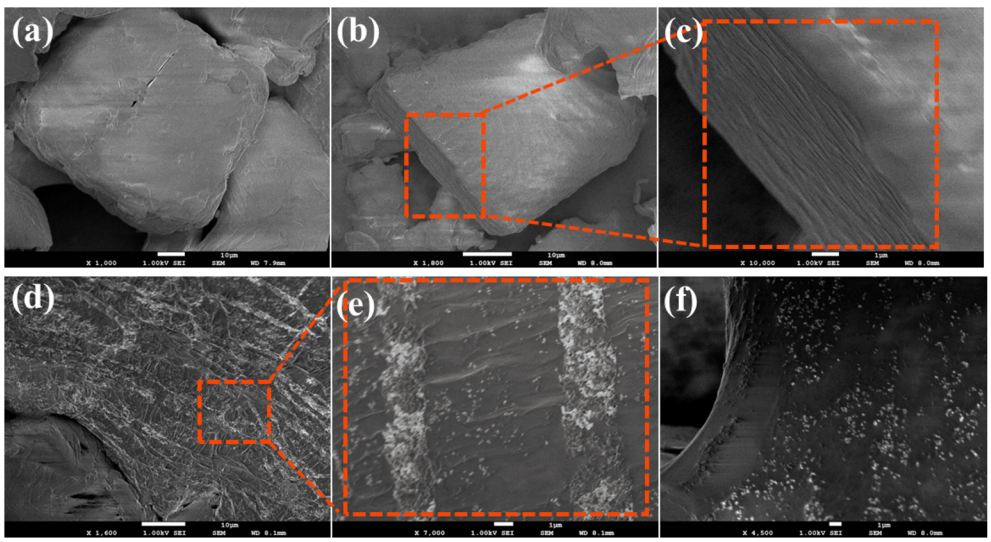

Fig. 10 Unoxidized PA6 material (a–c) and thermally oxidized PA6 material at 150 °C for 20 hours (d–f).

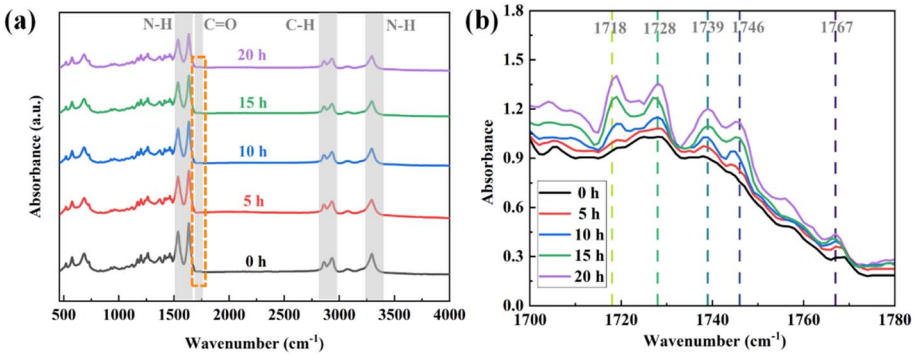

Fig. 11 FTIR spectral bands (a) and carbonyl growth (b) for a thermal oxidation temperature of 150 °C.

material remains consistent in the context of short-term thermal oxidation.

To illustrate the changes in the intensity of the carbonyl band at 1710–1780 cm^{-1}, this study conducted a detailed analysis of the carbonyl index for five peaks of the carbonyl band (C═O stretching vibration) that showed an increasing trend. These five absorption peaks are 1718 cm^{-1} (ketone), 1728 cm^{-1} (aldehyde), 1739 cm^{-1} (ester), 1746 cm^{-1} (aliphatic hydroxy acid), and 1767 cm^{-1} (isolated hydroxy acid). The trends in the carbonyl index of these absorption peaks at different thermal oxidation durations (5 h, 10 h, 15 h, and 20 h) with changing temperatures are shown in Fig. 12.

As the temperature increases, the carbonyl index of all carbonyl absorption peaks gradually rises, particularly when the temperature exceeds 120 °C, where the increase in the carbonyl index becomes more pronounced. This upward trend indicates that the thermal oxidation reaction intensifies with increasing temperature, accelerating the oxidation of PA6 at higher temperatures and leading to a significant increase in carbonyl content. The absorption peaks at 1718 cm^{-1} and 1728 cm^{-1} maintain relatively high carbonyl indices across the entire

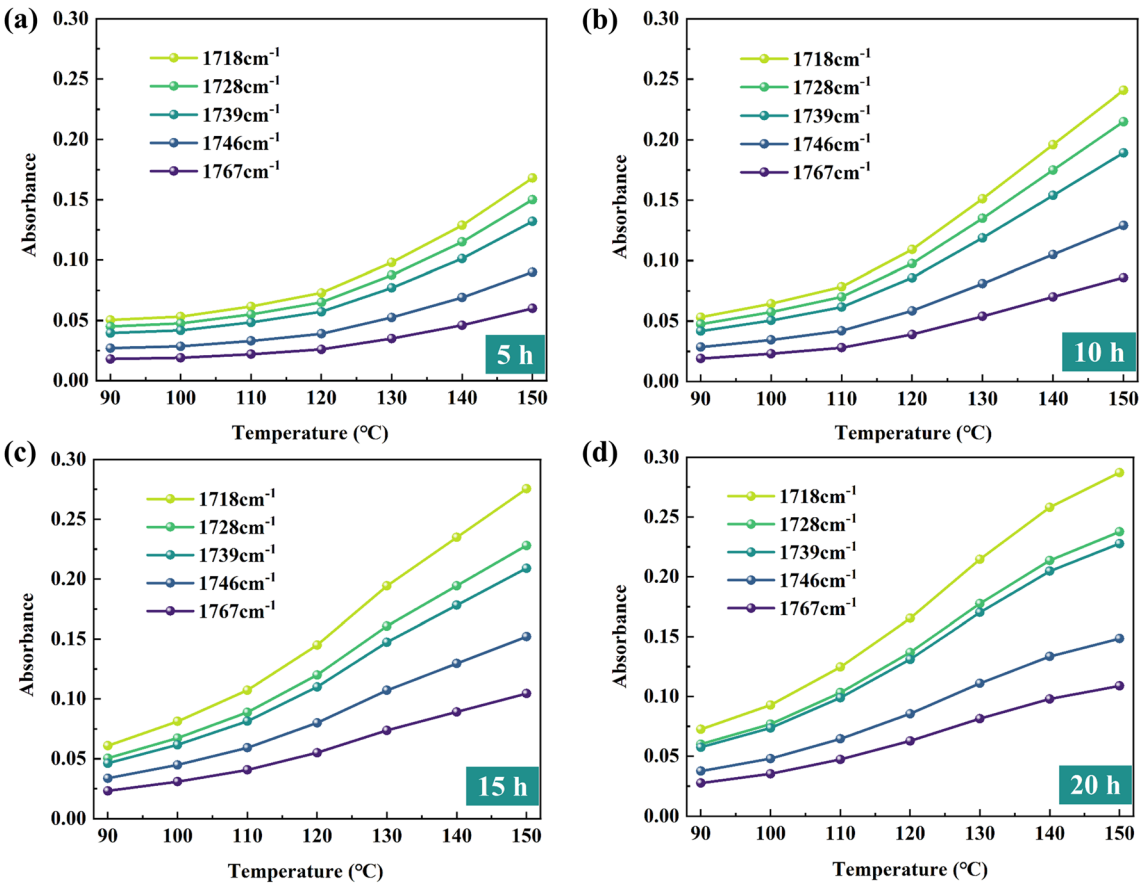

Fig. 12 Carbonyl index of PA6 materials with different thermal oxidation conditions (a–d).

temperature range, indicating that ketones and aldehydes gradually accumulate during the thermal oxidation process.

As the oxidation time extends from 5 hours to 20 hours, the carbonyl index under all temperature conditions continues to increase, especially in the high-temperature range (>130 °C), where the increase is particularly pronounced. This suggests that oxidation time plays a crucial role in the degree of oxidation of the material, with longer oxidation times leading to a higher degree of oxidation, resulting in more pronounced carbonyl formation. The carbonyl indices for the absorption peaks at 1718 cm^{-1} and 1728 cm^{-1} are consistently higher than those of other peaks across all time durations, indicating that these types of carbonyl groups are more easily formed and in larger quantities, making them the primary oxidation products during the thermal oxidation of PA6. With increasing time, the carbonyl indices for other absorption peaks (such as 1739 cm^{-1}, 1746 cm^{-1}, and 1767 cm^{-1}) also increase gradually, indicating the continuous accumulation of secondary oxidation products.

The synchronous increase in the intensity of carbonyl absorption peaks with time and temperature suggests that the formation of carbonyl groups is positively correlated with both temperature and oxidation duration. High temperatures and prolonged oxidation significantly raise the carbonyl index, reflecting an accelerated oxidation rate under these conditions. The results indicate that, under thermal oxidation conditions, the rate of carbonyl formation in PA6 increases significantly with temperature and oxidation time, with aldehydes and ketones showing the fastest growth rates. The observed trends in carbonyl index evolution demonstrate notable alignment with the foundational work of Shi *et al.*,[31] while strategically diverging in temporal scope. Where Shi's investigation prioritized prolonged oxidation durations to capture terminal degradation states, our study deliberately focuses on the nascent phase of thermal oxidation in PA6 materials, thereby addressing a critical knowledge gap regarding early-stage oxidative transformation kinetics.

Table 3 Characteristic points of TG and DTG curves for PA6 materials with different thermal oxidation conditions

Thermal oxidation condition	$T_{d5\%}$[a] (°C)	T_{dmax}[b] (°C)	T_{end}[c] (°C)
Unoxidized	378.67	447.67	480.83
150 °C, 20 h	361.67	441.55	476.8

[a] The temperature corresponding to a 5% mass loss is defined here as the initial decomposition temperature. [b] The peak point of the mass loss rate. [c] The DTG decomposition is considered complete when the absolute value of DTG is ≤0.02%.

3.5 Thermal performance analysis

3.5.1 TGA. To evaluate the effect of thermal oxidation on the thermal stability of PA6 material, thermogravimetric analysis (TGA) and derivative thermogravimetric analysis (DTG) were conducted on PA6 samples under different thermal oxidation conditions, and key temperature parameters were analyzed, as shown in Table 3.

Fig. 13(a) shows the TGA curves for PA6 samples thermally oxidized at 150 °C for 0, 5, 10, 15, and 20 hours. With increasing thermal oxidation time, the initial decomposition temperature ($T_{d5\%}$) of the material shows a clear downward trend, decreasing from 378.67 °C for unoxidized material to 361.67 °C. This change indicates that thermal oxidation significantly reduces the thermal stability of PA6, primarily due to the chain scission of polymer molecules and the formation of oxidation products during thermal oxidation. The DTG curves show that, at 150 °C, as the thermal oxidation time increases from 5 hours to 20 hours, the temperature corresponding to the maximum decomposition rate (T_{dmax}) also exhibits a noticeable decline (Fig. 13(b)). For unoxidized PA6, the maximum decomposition rate occurs at 447.67 °C, whereas for PA6 oxidized at 150 °C for 20 hours, the maximum decomposition rate decreases to 441.55 °C. The reduction in the peak temperature of the decomposition rate indicates that thermal oxidation accelerates the degradation of PA6, causing the material to begin decomposing at lower temperatures.

To reveal the effect of different thermal oxidation conditions on the thermal properties of PA6 material, a more in-depth analysis of the key temperature parameters was conducted. As the thermal oxidation temperature increased, the initial decomposition temperature ($T_{d5\%}$) of PA6 material showed

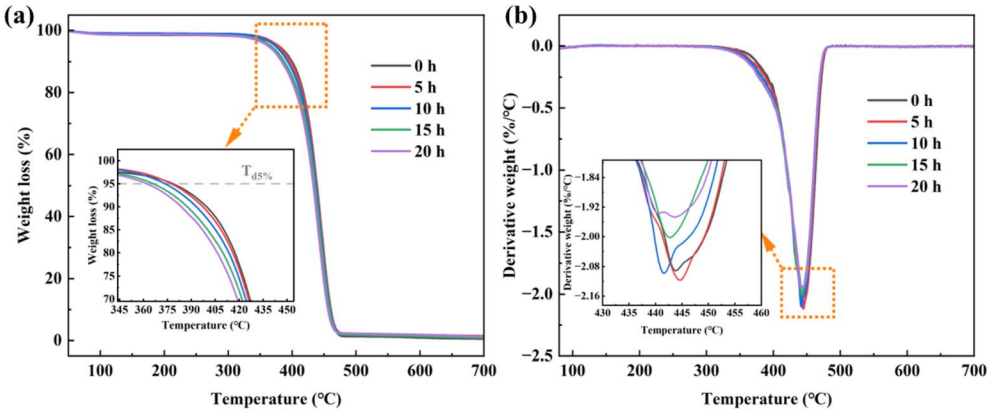

Fig. 13 (a) TGA and (b) DTG curves of PA6 materials under thermal oxidation at 150 °C.

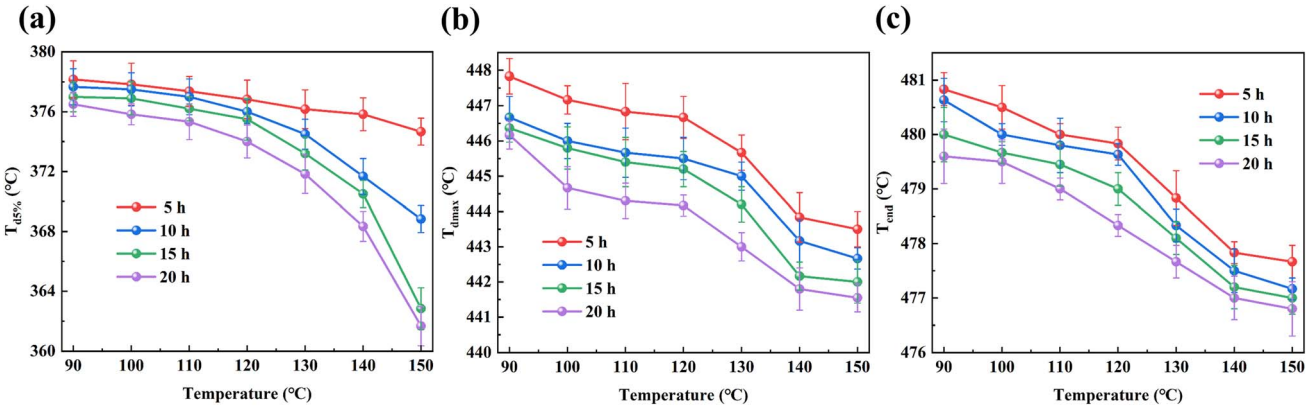

Fig. 14 Variation of pyrolysis temperature (a–c) of PA6 materials under different thermal oxidation conditions.

a decreasing trend. When the oxidation time was 5 hours, $T_{d5\%}$ decreased from 378.167 °C to 374.667 °C, a reduction of 3.5 °C. When the oxidation time was 10 hours, $T_{d5\%}$ decreased from 377.667 °C to 368.833 °C, a reduction of 8.83 °C. When the oxidation time was 15 hours, $T_{d5\%}$ decreased from 377 °C to 362.833 °C, representing a decrease of 14.17 °C. Finally, when the oxidation time was 20 hours, $T_{d5\%}$ decreased from 376.5 °C to 361.667 °C, a reduction of 14.83 °C. As seen from the $T_{d5\%}$ curve (Fig. 14(a)), $T_{d5\%}$ shows a distinct downward trend with increasing thermal oxidation time (5, 10, 15, 20 hours), indicating that the initial thermal decomposition temperature of the material gradually decreases. As the oxidation temperature increased from 90 °C to 150 °C, $T_{d5\%}$ decreased for all oxidation times, showing that thermal oxidation temperature has a significant effect on the initial stage of thermal decomposition of the material. Particularly at high temperatures (150 °C), prolonged thermal oxidation led to pronounced degradation, causing the material to begin thermal weight loss at lower temperatures.

As shown in Fig. 14(b), the T_{dmax} curve reveals that T_{dmax} decreases significantly with increasing thermal oxidation time, particularly under higher thermal oxidation temperatures (150 °C), where the 20 hour sample shows the lowest T_{dmax}. As the thermal oxidation temperature increases, T_{dmax} decreases by 4.3 °C, 4.0 °C, 4.4 °C, and 4.6 °C for oxidation times of 5, 10, 15, and 20 hours, respectively, with the rate of decrease in maximum decomposition temperature being relatively consistent. This indicates that prolonged thermal oxidation (15–20 hours) causes the peak decomposition rate to occur at lower temperatures, implying that thermal oxidation accelerates the degradation of the material, reducing its thermal stability. Additionally, an increase in oxidation temperature also leads to a reduction in the temperature corresponding to the maximum weight loss rate.

As shown in Fig. 14(c), the T_{end} curve represents the ending temperature of the decomposition process. With increasing thermal oxidation time, T_{end} gradually decreases. Under 20 hours of thermal oxidation, the material exhibits the lowest decomposition ending temperature, indicating that the completion point of degradation occurs earlier, and the material's thermal resistance further declines. As the oxidation temperature increases from 90 °C to 150 °C, the T_{end} values of all samples show a decreasing trend, which is consistent with the TGA and DTG analyses, demonstrating the overall negative impact of thermal oxidation on the decomposition process of the material.

In summary, it can be concluded that thermal oxidation significantly reduces the thermal stability of PA6. This is evidenced by the decrease in the initial decomposition temperature ($T_{d5\%}$), the peak decomposition rate temperature (T_{dmax}), and the end decomposition temperature (T_{end}) as thermal oxidation time increases. These results indicate that after prolonged thermal oxidation, particularly at 20 hours, the molecular chain structure of PA6 is damaged, resulting in an overall reduction in decomposition temperatures. Thermal oxidation leads to oxidative degradation and possible crosslinking reactions within PA6 molecular chains, generating oxidation products such as carbonyl groups. These chemical changes result in polymer chain scission, lowering the average molecular weight of the material and reducing its thermal stability and high-temperature resistance. The reduction in decomposition peaks and the advancement of the thermal decomposition process suggest that the material becomes more prone to degradation. Under different thermal oxidation temperature conditions, the thermal stability of all samples (as indicated by $T_{d5\%}$, T_{dmax}, and T_{end}) decreases with increasing oxidation temperature, indicating that higher temperatures promote the thermal oxidation process. This trend is particularly pronounced under long-term thermal oxidation (20 hours), demonstrating that the interaction between temperature and time significantly accelerates the oxidative degradation of PA6.

3.5.2 DSC. To analyze the crystallization and melting behavior of unoxidized and oxidized PA6 material, a detailed discussion and analysis were conducted on the test results of PA6 materials at different thermal oxidation times.

The relationship between the melting peak temperature (T_m) of PA6 material and thermal oxidation time and temperature is shown in Fig. 15(a). The melting peak temperature (T_m) of PA6 continuously decreases with increasing oxidation time and treatment temperature, while the initial melting temperature

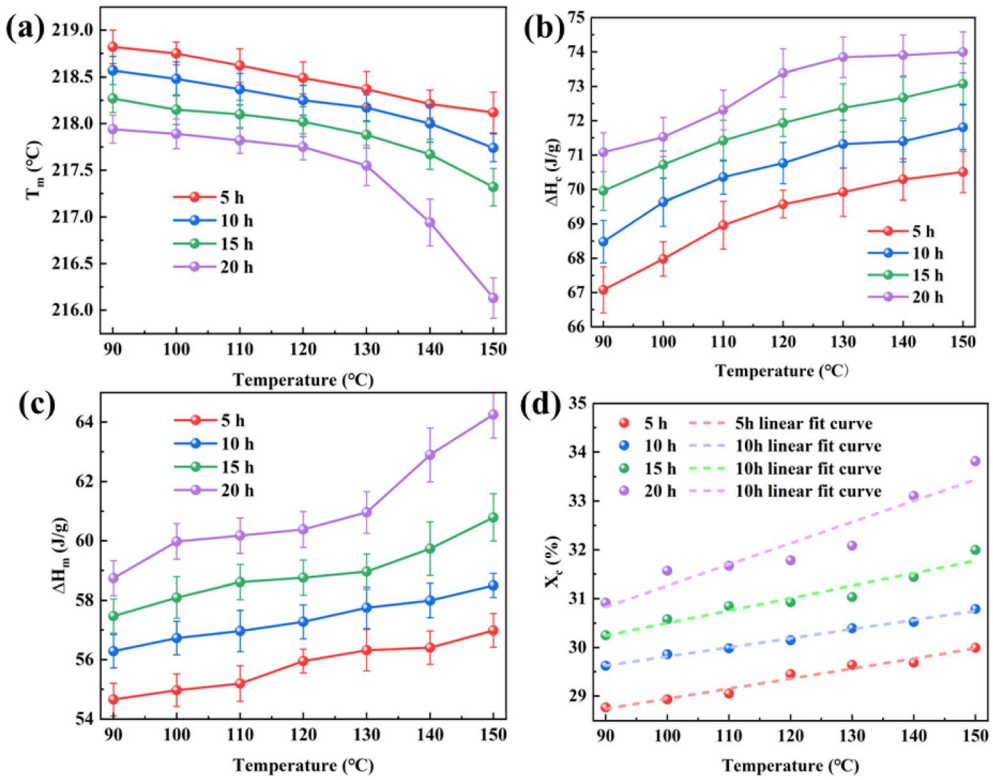

Fig. 15 (a) Melting peak, (b) enthalpy of crystallization, (c) enthalpy of fusion and (d) degree of crystallinity of PA6 materials under different thermal oxidation conditions.

(T_i) decreases, and the melting peak width (ΔW_m) widens (Table 4). This trend was observed in all samples regardless of oxidation time, indicating that the thermal oxidation degradation process significantly affects the crystallization properties of PA6 material. Specifically, the decrease in T_m is more pronounced in samples subjected to longer thermal oxidation times (15 hours and 20 hours) compared to those treated for shorter periods (5 hours and 10 hours). For samples oxidized for 5 hours, T_m remained relatively high compared to other groups, with only a slight decrease from approximately 218.82 °C at 90 °C to 218.12 °C at 150 °C. However, for samples treated for a longer oxidation time (20 hours), a more significant reduction in T_m was observed, decreasing from 217.94 °C at 90 °C to 216.13 °C at 150 °C as the treatment temperature increased.

The relationship between the melting enthalpy (ΔH_m) of PA6 material and temperature shows that ΔH_m exhibits different trends with increasing oxidation time and treatment temperature (Fig. 15(c)). For samples oxidized for 5 hours, ΔH_m increased from 54.65 J g^{-1} at 90 °C to 56.98 J g^{-1} at 150 °C, indicating an improvement in the crystallinity of PA6 under short oxidation times. However, as the oxidation time extended to 20 hours, ΔH_m increased from 58.74 J g^{-1} at 90 °C to 64.25 J g^{-1} at 150 °C, suggesting a more pronounced effect of oxidation on the internal structure of the material. This may be due to partial reorganization and increased crystallinity in the amorphous regions during prolonged oxidation. The increase in ΔH_m reflects changes in the degree of crystallinity (X_c) of the material during thermal oxidation (Fig. 15(d)). From the linear fitting curve of X_c for different oxidation times, it is evident that X_c of PA6 gradually increases with rising oxidation temperatures, and the longer the oxidation time, the more pronounced the increase in crystallinity. This increase in crystallinity may be attributed to recrystallization occurring in some amorphous regions during thermal oxidation, leading to an increase in material order. Therefore, as temperature and oxidation time increase, the increase in crystallinity reflects the gradual reorganization and ordering of the material's internal structure, especially for samples oxidized for 20 hours. The significant increase in ΔH_m and X_c indicates that the material undergoes complex physical and chemical changes in an oxidative

Table 4 Critical DSC values for unoxidized and oxidized PA6 materials

Thermal oxidation condition	T_i (°C)	T_m (°C)	ΔW_m (°C)	T_c (°C)	ΔH_m (J g^{-1})	ΔH_c (J g^{-1})	X_c (%)
Unoxidized	208.10	218.95	15.55	182.96	54.02	67.08	28.43
150 °C, 20 h	207.35	216.13	17.07	185.41	64.24	73.99	33.82

environment. This trend is consistent with the changes in ΔH_m, further demonstrating the significant impact of thermal oxidation on the structure and properties of PA6.

Fig. 15(b) shows the relationship between the crystallization enthalpy (ΔH_c) of PA6 material and temperature for thermal oxidation times of 5, 10, 15, and 20 hours. It can be observed that as the temperature increases and the thermal oxidation time extends, ΔH_c gradually increases, and the crystallization peak temperature (T_c) also shifts to higher temperatures (Table 4). For samples oxidized for 5 hours, ΔH_c increased from 67.08 J g^{-1} at 90 °C to 70.5 J g^{-1} at 150 °C. For samples oxidized for 20 hours, ΔH_c increased from 71.08 J g^{-1} at 90 °C to 73.99 J g^{-1} at 150 °C. This trend indicates that as the temperature and thermal oxidation time increase, ΔH_c of PA6 continues to increase. However, when the oxidation time reaches 20 hours and the oxidation temperature exceeds 120 °C, the increasing trend of ΔH_c begins to level off. The increase in ΔH_c reflects changes in the internal structure of the material during thermal oxidation, particularly the growth of crystalline regions. This trend is consistent with the changes in ΔH_m and X_c, further supporting the conclusion that the material's structure becomes more ordered during thermal oxidation. These changes suggest that the molecular chains of PA6 undergo rearrangement under thermal oxidation conditions, with some amorphous regions transforming into crystalline regions, thereby increasing ΔH_m and X_c. This observation aligns with the seminal findings of Shu *et al.*[29] in their early investigations of PA6 aging, where prolonged aging durations were correlated with increased crystallinity and concomitant reductions in melting peak temperature. The consistency across studies reinforces the universality of these aging-induced structural transformations in polyamide systems, while our work extends the conceptual framework through mechanistic reinterpretation.

These results indicate that PA6 is highly sensitive to thermal oxidation, emphasizing the influence of oxidation duration and temperature on its thermal and crystallization properties. The findings suggest that in applications involving prolonged exposure to high temperatures, managing thermal conditions and controlling the oxidative environment are crucial for maintaining the thermal stability of PA6.

4 Conclusion

In this study, the mechanical and thermal properties of PA6 material under short-term thermal oxidation were investigated by controlling the oxidation duration. The tensile test results indicate that under short-term thermal oxidation, stiffness remained relatively unaffected, while the tensile strength initially showed a gradual increase, followed by a significant decline at higher temperatures. Ductility continuously decreased until it ultimately exhibited brittle fracture under thermal oxidation at 150 °C. When the oxidation temperature exceeded 130 °C, the bending strength showed a sharp decline, and the longer the oxidation time, the more pronounced the decrease in bending strength. The bending modulus exhibited a trend of first increasing and then decreasing with increasing oxidation temperature, reaching its maximum value at an oxidation temperature of 130 °C and an oxidation duration of 10 hours. The impact strength showed a clear and continuous decline with increasing oxidation temperature.

Infrared analysis of PA6 under thermal oxidation indicated that the rate of carbonyl formation significantly increased with higher temperatures and longer oxidation times, with aldehydes and ketones showing the fastest growth rates. High temperatures and prolonged thermal oxidation had a significant effect on the chemical structure and mechanical properties of the material, providing essential theoretical support for understanding the thermal aging behavior and durability of the material.

PA6 material undergoes significant thermal degradation under high-temperature thermal oxidation, with its thermal stability decreasing with longer oxidation times and higher temperatures. Prolonged (*e.g.*, 20 hours) and high-temperature (*e.g.*, 150 °C) thermal oxidation led to a significant decrease in the initial decomposition temperature, maximum weight loss rate temperature, and end decomposition temperature, reflecting damage to the material's microstructure due to thermal oxidation. With increasing oxidation time and temperature, the melting temperature of PA6 decreased significantly, while melting enthalpy, crystallinity, and crystallization enthalpy gradually increased, indicating processes of chain scission, recrystallization, and structural ordering during thermal oxidation. The results show that PA6 is highly sensitive to thermal oxidation, which enhances crystallization properties while reducing melting temperature.

For Type IV hydrogen storage cylinders, it is essential to fully consider the impact of thermal oxidation on mechanical properties and thermal stability. The thermal curing process for epoxy resin used in carbon fiber winding should not involve excessively high curing temperatures, as high temperatures or prolonged curing times can adversely affect the stability and mechanical properties of the liner material, ultimately reducing its service life. For PA6 material used under high-temperature and prolonged exposure conditions, ensuring its applicability and safety is critical. In material modification and practical applications, it may be necessary to introduce antioxidants or select materials with higher thermal stability to mitigate the degradation process due to thermal oxidation.

Data availability

The data that support the findings of this study are available from the corresponding author, [Q. Wang], upon reasonable request.

Conflicts of interest

The authors declare no competing financial interests.

Acknowledgements

Jilin Science and Technology Innovation Development Program Project, China (No. 20230401005).

References

1 C. P. Sahwal, S. Sengupta and T. Q. Dinh, Advanced Equivalent Consumption Minimization Strategy for Fuel Cell Hybrid Electric Vehicles, *J. Cleaner Prod.*, 2024, **437**, 140366, DOI: 10.1016/j.jclepro.2023.140366.

2 A. Veziroglu and R. Macario, Fuel cell vehicles: State of the art with economic and environmental concerns, *Int. J. Hydrogen Energy*, 2011, **36**(1), 25–43, DOI: 10.1016/j.ijhydene.2010.08.145.

3 A. Midilli and I. Dincer, Hydrogen as a renewable and sustainable solution in reducing global fossil fuel consumption, *Int. J. Hydrogen Energy*, 2008, **33**(16), 4209–4222, DOI: 10.1016/j.ijhydene.2008.05.024.

4 S. Sapre, K. Pareek, R. Rohan and P. K. Singh, H2 refueling assessment of composite storage tank for fuel cell vehicle, *Int. J. Hydrogen Energy*, 2019, **44**(42), 23699–23707, DOI: 10.1016/j.ijhydene.2019.07.044.

5 M. Yue, H. Lambert, E. Pahon, R. Roche, S. Jemei and D. Hissel, Hydrogen energy systems: A critical review of technologies, applications, trends and challenges, *Renewable Sustainable Energy Rev.*, 2021, **146**, 111180, DOI: 10.1016/j.rser.2021.111180.

6 Y. Zhao, G. Chen, Q. Xu, H. Lv, S. Su, L. Xia, G. Zhang, G. Yang and K. Hu, Metering inaccuracy analysis and improvement measures of typical scenarios in hydrogen refueling station, *Int. J. Hydrogen Energy*, 2024, **50**, 815–828, DOI: 10.1016/j.ijhydene.2023.07.101.

7 M. R. Usman, Hydrogen storage methods: Review and current status, *Renewable Sustainable Energy Rev.*, 2022, **167**, 112743, DOI: 10.1016/j.rser.2022.112743.

8 A. María Villarreal Vives, R. Wang, S. Roy and A. Smallbone, Techno-economic analysis of large-scale green hydrogen production and storage, *Appl. Energy*, 2023, **346**(15), 121333, DOI: 10.1016/j.apenergy.2023.121333.

9 X. Li, Q. Huang, Y. Liu, B. Zhao and J. Li, Review of the Hydrogen Permeation Test of the Polymer Liner Material of Type IV On-Board Hydrogen Storage Cylinders, *Materials*, 2023, **16**(15), 5366, DOI: 10.3390/ma16155366.

10 C. Dong, Y. Liu, J. Li, G. Bin, C. Zhou, W. Han and X. Li, Hydrogen Permeability of Polyamide 6 Used as Liner Material for Type IV On-Board Hydrogen Storage Cylinders, *Polymers*, 2023, **15**(18), 3715, DOI: 10.3390/polym15183715.

11 H. Fujiwara, H. Ono, K. Onoue and S. Nishimura, High-pressure gaseous hydrogen permeation test method -property of polymeric materials for high-pressure hydrogen devices (1), *Int. J. Hydrogen Energy*, 2020, **45**(53), 29082–29094, DOI: 10.1016/j.ijhydene.2020.07.215.

12 P. Sharma, S. Sharma, T. Bera, K. Semwal, R. M. Badhe, A. Sharma, G. S. Kapur, S. S. V. Ramakumar and S. Neogi, Effects of dome shape on burst and weight performance of a type-3 composite pressure vessel for storage of compressed hydrogen, *Compos. Struct.*, 2022, **293**, 115732, DOI: 10.1016/j.compstruct.2022.115732.

13 W. Zhou, J. Wang, Z.-b. Pan, J. Liu, L.-h. Ma, J.-y. Zhou and Y.-f. Su, Review on optimization design, failure analysis and non-destructive testing of composite hydrogen storage vessel, *Int. J. Hydrogen Energy*, 2022, **47**(91), 38862–38883, DOI: 10.1016/j.ijhydene.2022.09.028.

14 J. Pepin, E. Lainé, J.-C. Grandidier, S. Castagnet, P. Blanc-vannet, P. Papin and M. Weber, Determination of key parameters responsible for polymeric liner collapse in hyperbaric type IV hydrogen storage vessels, *Int. J. Hydrogen Energy*, 2018, **43**(33), 16386–16399, DOI: 10.1016/j.ijhydene.2018.06.177.

15 J. Hu and K. Chandrashekhara, Fracture analysis of hydrogen storage composite cylinders with liner crack accounting for autofrettage effect, *Int. J. Hydrogen Energy*, 2009, **34**(8), 3425–3435, DOI: 10.1016/j.ijhydene.2009.01.094.

16 T. A. Yersak, D. R. Baker, Y. Yanagisawa, S. Slavik, R. Immel, A. Mack-Gardner, M. Herrmann and M. Cai, Predictive model for depressurization-induced blistering of type IV tank liners for hydrogen storage, *Int. J. Hydrogen Energy*, 2017, **42**(48), 28910–28917, DOI: 10.1016/j.ijhydene.2017.10.024.

17 M. Nouri, F. A. Ghasemi, G. R. Sherbaf and K. R. Kashyzadeh, Fatigue Analysis of a Type-IV CNG Composite Cylinder with Variable Wall-Thickness and Polyethylene Liner, *Mech. Compos. Mater.*, 2023, **59**, 927–944, DOI: 10.1007/s11029-023-10143-5.

18 J. Zhang, L. Lei, W. Zhou, G. Li, Y. Yan and Z. Ni, Cryogenic mechanical and hydrogen-barrier properties of carbon fiber composites for type V cryo-compressed hydrogen storage vessels, *Compos. Commun.*, 2023, **43**, 101733, DOI: 10.1016/j.coco.2023.101733.

19 X. Wang, M. Tian, X. Chen, P. Xie, J. Yang, J. Chen and W. Yang, Advances on materials design and manufacture technology of plastic liner of type IV hydrogen storage vessel, *Int. J. Hydrogen Energy*, 2022, **47**(13), 8382–8408, DOI: 10.1016/j.ijhydene.2021.12.198.

20 S. Sathees Kumar and G. Kanagaraj, Investigation on Mechanical and Tribological Behaviors of PA6 and Graphite-Reinforced PA6 Polymer Composites, *Arabian J. Sci. Eng.*, 2016, **41**(11), 4347–4357, DOI: 10.1007/s13369-016-2126-2.

21 S. Marais, Q. Lozay, N. Follain, J. Soulestin, N. Couvrat and E. Dargent, Multinanolayered PA6/Cloisite and PE/PA6/Cloisite composites: Structure, mechanical and barrier properties, *Composites, Part B*, 2024, **271**, 111167, DOI: 10.1016/j.compositesb.2023.111167.

22 D. Lellinger, I. Alig, H. Oehler, K. Rode, F. Malz, L. M. Herkenrath and J. Y. Youn, Accelerated thermal aging of thermoplastic materials for the motor compartment: Characterization, degradation model and lifetime prediction, *Service Life Prediction of Polymers and Coatings*, 2020, pp. 117–161, DOI: 10.1016/b978-0-12-818367-0.00008-4.

23 P. Gijsman, G. Hensen and M. Mak, Thermal initiation of the oxidation of thermoplastic polymers (Polyamides, Polyesters and UHMwPE), *Polym. Degrad. Stab.*, 2021, **183**, 109452, DOI: 10.1016/j.polymdegradstab.2020.109452.

24 E. Richaud, O. Okamba Diogo, B. Fayolle, J. Verdu, J. Guilment and F. Fernagut, Review: Auto-oxidation of

aliphatic polyamides, *Polym. Degrad. Stab.*, 2013, **98**(9), 1929–1939, DOI: **10.1016/j.polymdegradstab.2013.04.012**.

25 F. Zhang, R. Yang and D. Lu, Investigation of Polymer Aging Mechanisms Using Molecular Simulations: A Review, *Polymer*, 2023, **15**(8), 1928, DOI: **10.3390/polym15081928**.

26 X.-F. Wei, K. J. Kallio, S. Bruder, M. Bellander, H.-H. Kausch, U. W. Gedde and M. S. Hedenqvist, Diffusion-limited oxidation of polyamide: Three stages of fracture behavior, *Polym. Degrad. Stab.*, 2018, **154**, 73–83, DOI: **10.1016/j.polymdegradstab.2018.05.024**.

27 D. Forsström and B. Terselius, Thermo oxidative stability of polyamide 6 films I. Mechanical and chemical characterisation, *Polym. Degrad. Stab.*, 2000, **67**(1), 69–78, DOI: **10.1016/s0141-3910(99)00122-6**.

28 L. Rongfu and H. Xingzhou, Study on discoloration mechanism of polyamide 6 during thermo-oxidative degradation, *Polym. Degrad. Stab.*, 1998, **62**, 523–528.

29 Y. Shu, L. Ye and T. Yang, Study on the long-term thermal-oxidative aging behavior of polyamide 6, *J. Appl. Polym. Sci.*, 2008, **110**(2), 945–957, DOI: **10.1002/app.28647**.

30 W. Dong and P. Gijsman, Influence of temperature on the thermo-oxidative degradation of polyamide 6 films, *Polym. Degrad. Stab.*, 2010, **95**(6), 1054–1062, DOI: **10.1016/j.polymdegradstab.2010.02.030**.

31 K. Shi, L. Ye and G. Li, Thermal oxidative aging behavior and stabilizing mechanism of highly oriented polyamide 6, *J. Therm. Anal. Calorim.*, 2016, **126**(2), 795–805, DOI: **10.1007/s10973-016-5523-6**.

32 M. Pliquet, M. Rapeaux, F. Delange, P. O. Bussiere, S. Therias and J. L. Gardette, Multiscale analysis of the thermal degradation of polyamide 6,6: Correlating chemical structure to mechanical properties, *Polym. Degrad. Stab.*, 2021, **185**, 109496, DOI: **10.1016/j.polymdegradstab.2021.109496**.

33 X. Wang, X. Chen, J. Yang, P. Xie and W. Yang, Research on torsional laminated extrusion for improving the permeability and mechanical properties of HDPE/PA6 composite for type IV storage tank liners, *J. Appl. Polym. Sci.*, 2023, **140**(42), 54567, DOI: **10.1002/app.54567**.

34 F. Alexis, S. Castagnet, C. Nadot-Martin, G. Robert and P. Havet, Effect of severe thermo-oxidative aging on the mechanical behavior and fatigue durability of short glass fiber reinforced PA6/6.6, *Int. J. Fatigue*, 2023, **166**, 107280, DOI: **10.1016/j.ijfatigue.2022.107280**.

35 S. Backens, J. Siering, S. Schmidt, N. Glück and W. Flügge, Comparative study of thermoplastic liner materials with regard to mechanical and permeation barrier properties before and after cyclic thermal aging, *Mater. Test.*, 2021, **63**(4), 311–316, DOI: **10.1515/mt-2020-0051**.